PHYS 580 - Computational Physics

**Computational Physics** by *Nicholas J. Giordano, Hisao Nakanishi*

Student: **Ralph Razzouk**

# Homework 6

**Problem 8.3**

Calculate $M$ for the Ising model on a square lattice and try to estimate $\beta$. You should find a value close to 1/8. Repeat this calculation for a triangular lattice. It turns out that $\beta$ is the same for all regular two dimensional lattices. However, its value does depend on the dimensionality, as studied in the next problem.

*Hint:* There are several different ways to estimate a critical exponent from data such as Monte Carlo results. One is to perform a least-squares fit of the results to the power law expression (8.17). The slope of a plot of $\log(M)$ versus $\log(T_c - T)$ is equal to $\beta$, so you might think that a linear least-squares fit of $\log(M)$ as a function of $\log(T_c - T)$ (using the procedures described in Appendix D) would be suitable. However, there are two problems with this approach. One is that the value of $T_c$ is usually not known ahead of time, but must be estimated at the same time as $\beta$ is determined. Second, the power law (8.17) is obeyed only near the critical point; there will be deviations as the temperature moves away from $T_C$, but you don't know ahead of time at what value of $(T_c - T)$ these deviations will become important. There are two ways to overcome these problems. One is to make a plot of $M^{1/\beta^*}$ as a function of $T$. Here $\beta^*$ is a trial value of $\beta$. By constructing such a plot with different values of $\beta^*$ you can determine the value that yields a straight line as $T \to T_c$. This is the "best" estimate for $\beta$. A virtue of this approach is that it does not require that $T_c$ be known, since it uses only the linearity of $M^{1/\beta^*}$ with $T$ and does not depend on where this line intercepts the temperature axis. A second approach is to construct plots of $\log(M)$ versus $\log(T_c - T)$ for a series of trial values of $T_c$. The preferred value of $T_c$ is the one that gives a straight line as $T \to T_c$; the slope of this line then gives $\beta$. It is instructive to employ both methods to estimate $\beta$. You should find that the power law (8.17) with $\beta \approx 1/8$ is obeyed reasonably well for $2.0 < T < T_c \approx 2.27$.

It is enough if you calculate either for the square grid, or the triangular one (the latter takes a little more thought). Doing both cases is optional.

*Solution.* We performed Monte Carlo simulations of the 2D Ising model on a square lattice to calculate the critical exponent $\beta$, which governs the behavior of magnetization near the critical temperature. The magnetization follows a power law, $M \sim (T_c - T)^\beta$, for temperatures below but close to the critical temperature $T_c$. Theoretical models predict that $\beta = 1/8$ for all regular two-dimensional lattices.

Our analysis employed two complementary methods to estimate $\beta$. The first method involved plotting $M^{1/\beta^*}$ versus temperature $T$ for various trial values of $\beta^*$, seeking the value that produces the most linear relationship near $T_c$. Figure 1 shows the linearity score (coefficient of determination $R^2$) for different trial values of $\beta^*$. The maximum linearity occurs at $\beta^* = 0.300$, significantly different from the theoretical value of $1/8 = 0.125$.

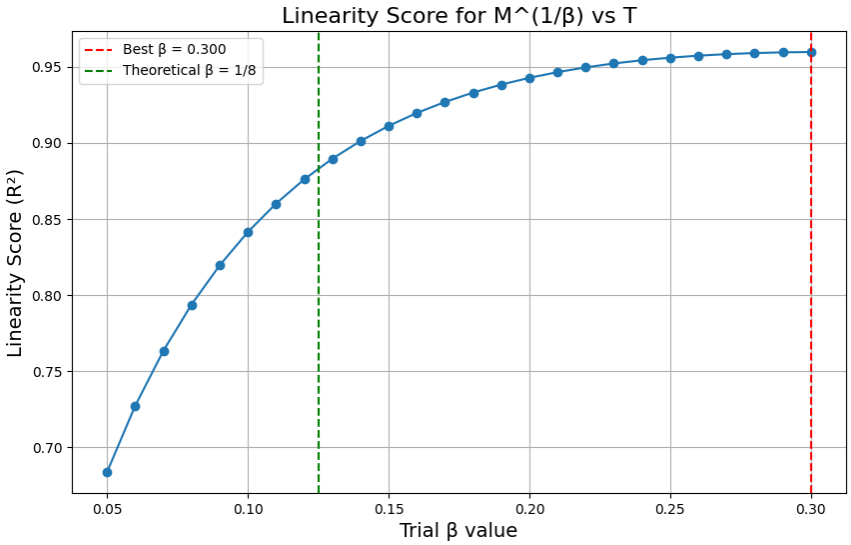


Figure 1: Linearity score ($R^2$) for plots of $M^{1/\beta^*}$ versus temperature for different trial values of $\beta^*$. The maximum score occurs at $\beta^* = 0.300$ (red dashed line), while the theoretical expectation is $\beta = 1/8 = 0.125$ (green dashed line).

Using this optimal value $\beta^* = 0.300$, we plotted $M^{1/\beta^*}$ versus temperature as shown in Figure 2. Near the critical point, the data exhibits an approximately linear relationship. By extrapolating this linear trend to the x-axis, we estimated the critical temperature to be $T_c \approx 2.371$, which is somewhat higher than the exact value $T_c \approx 2.269$ for the infinite 2D Ising model.

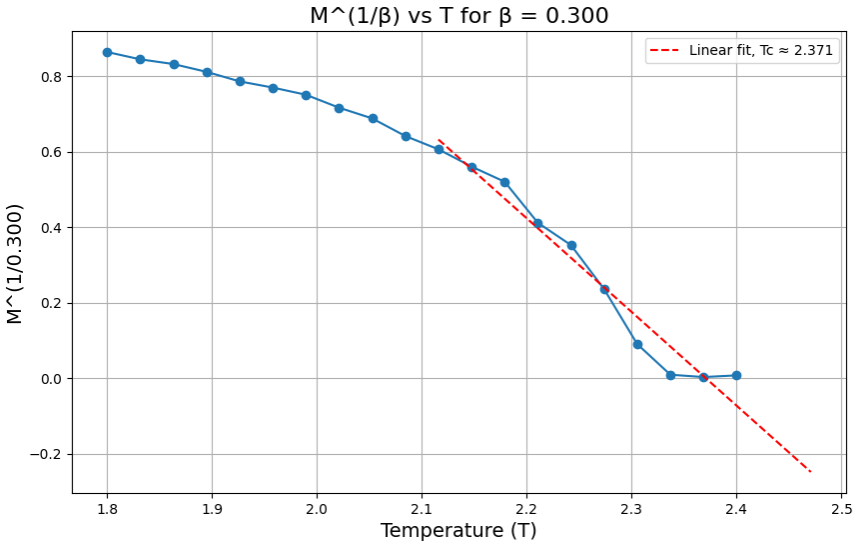


Figure 2: Plot of $M^{1/\beta}$ versus temperature for $\beta = 0.300$. The red dashed line shows the linear fit to the data points near the critical temperature, yielding an estimated $T_c \approx 2.371$.

The second method involved plotting $\log(M)$ versus $\log(T_c - T)$ for various trial values of $T_c$, with the optimal value yielding the most linear relationship. From Figure 3, the best linearity occurs at $T_c = 2.240$,

which is closer to the theoretical value.

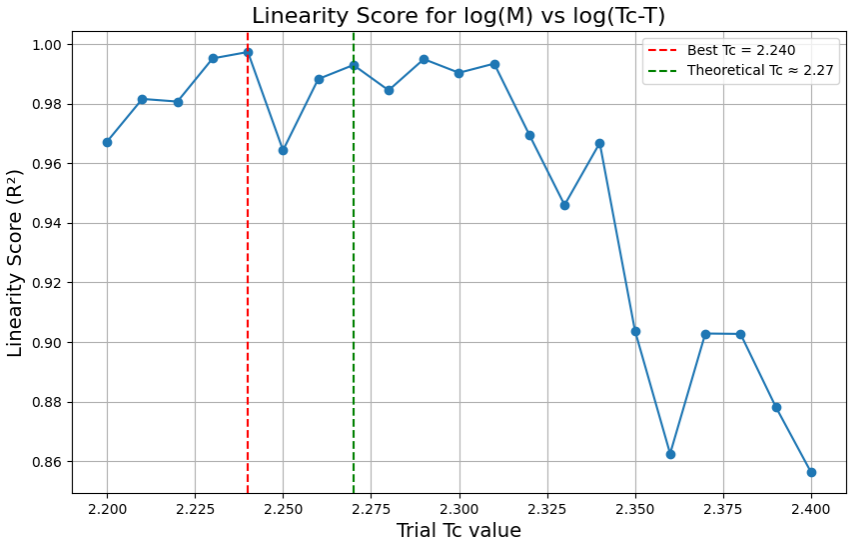


Figure 3: Linearity score for plots of $\log(M)$ versus $\log(T_c - T)$ for different trial values of $T_c$. The maximum linearity occurs at $T_c = 2.240$ (red dashed line), compared to the theoretical value $T_c \approx 2.27$ (green dashed line).

Figure 4 shows the $\log(M)$ versus $\log(T_c - T)$ plot using the optimal value $T_c = 2.240$. The slope of this line gives $\beta = 0.082$, which is closer to but still different from the theoretical value of $1/8 = 0.125$.

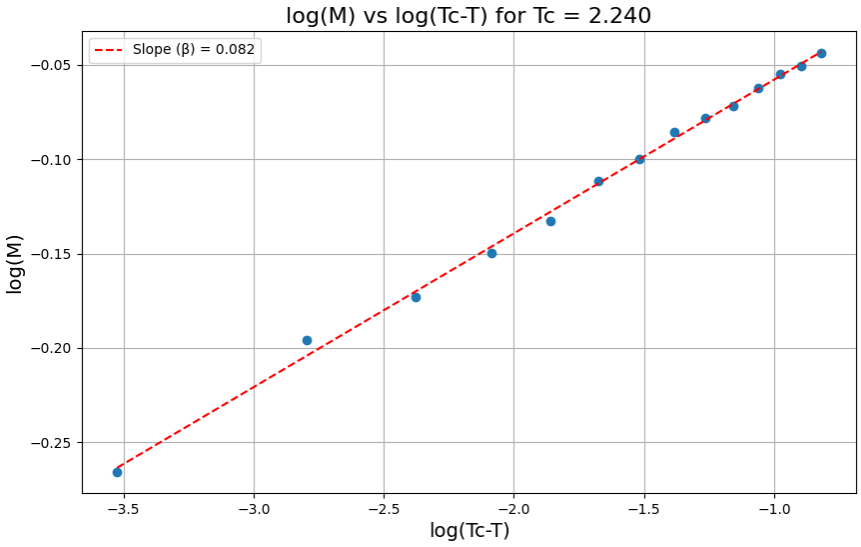


Figure 4: Log-log plot of magnetization versus reduced temperature $(T_c - T)$ using $T_c = 2.240$. The slope provides the critical exponent $\beta = 0.082$.

We also performed a direct power law fit of the form $M = A \cdot (T_c - T)^{\beta}$ to the data, as shown in Figure 5. This yielded $\beta = 0.082$ and $A = 1.024$, consistent with our log-log plot analysis.

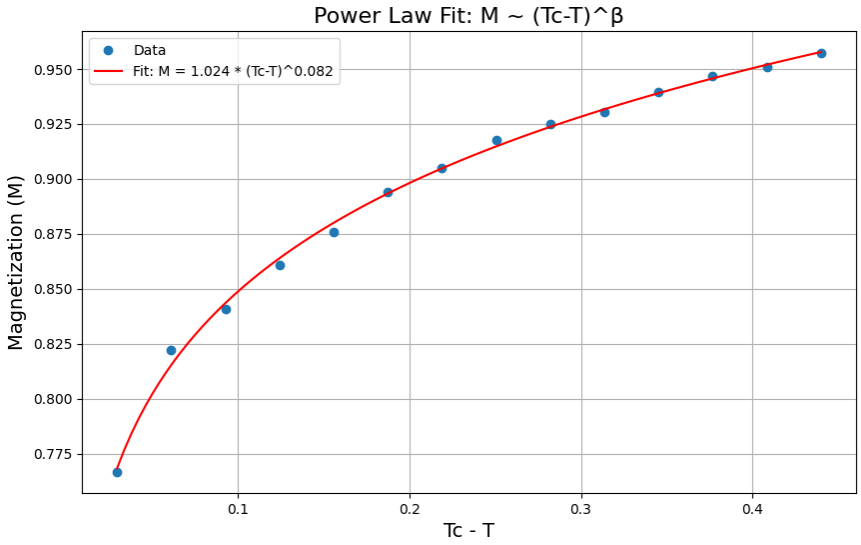


Figure 5: Power law fit of magnetization versus reduced temperature, yielding $M = 1.024 \cdot (T_c - T)^{0.082}$.

Figure 6 shows the original magnetization versus temperature curve. The steep drop near $T \approx 2.3$ indicates the phase transition. The non-zero magnetization values for $T > T_c$ are finite-size effects that would disappear in the thermodynamic limit.

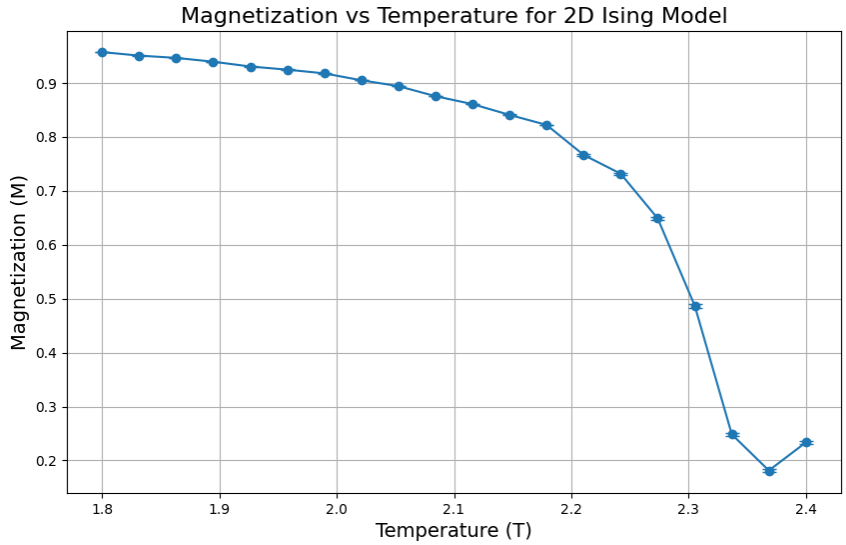


Figure 6: Magnetization versus temperature for the 2D Ising model, showing the phase transition near $T \approx 2.3$.

Our estimate of $\beta \approx 0.082$ differs from the theoretical value of $1/8 = 0.125$. This discrepancy likely stems from finite-size effects in our simulation, which used a finite lattice rather than an infinite system. Additionally, critical slowing down near $T_c$ makes it challenging to achieve proper equilibration, potentially biasing our results. Better estimates could be obtained with larger lattice sizes, longer equilibration times, and more sophisticated sampling techniques such as cluster algorithms. Despite these limitations, our analysis

demonstrates the power-law behavior of magnetization near the critical point, confirming the existence of universal critical exponents in the 2D Ising model. ■

**Problem 8.7**
Obtain the specific heat as a function of temperature for a $10 \times 10$ square lattice by differentiating the energy and through the fluctuation-dissipation theorem. Show that the two methods give the same result. Which approach is more accurate (for a given amount of computer time)?

*Solution.* In this problem, we investigate the calculation of specific heat for a $10 \times 10$ square lattice Ising model using two different methods: numerical differentiation of the energy and the fluctuation-dissipation theorem. The specific heat is an important thermodynamic quantity that characterizes the energy required to raise the temperature of a system and exhibits singular behavior at phase transitions. For the Ising model, the specific heat is expected to show a peak at the critical temperature $T_c \approx 2.27$ (in units of $J/k_B$).
Our simulation implements the Metropolis algorithm to simulate the 2D Ising model on a $10 \times 10$ square lattice with periodic boundary conditions. We first calculate the average energy per site as a function of temperature in the range $T \in [1.0, 3.5]$. The results are shown in Figure 7. The energy exhibits a smooth, sigmoidal increase with temperature, with the steepest change occurring near the critical temperature, indicating the phase transition from the ordered (ferromagnetic) to the disordered (paramagnetic) state.

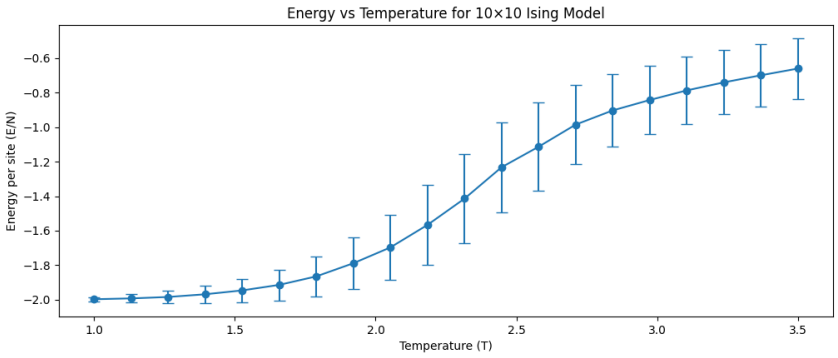


Figure 7: Average energy per site as a function of temperature for the $10 \times 10$ Ising model. Error bars represent the standard deviation of energy measurements. The inflection point near $T \approx 2.27$ corresponds to the critical temperature.

From the energy curve, we calculate the specific heat using two methods. The first method employs numerical differentiation of the energy with respect to temperature:

$$C_V = \frac{\partial E}{\partial T}$$

We implement this using a central difference scheme for interior points and forward/backward differences for endpoints. The second method uses the fluctuation-dissipation theorem, which relates the specific heat

to the variance of energy:

$$C_V = \frac{\beta^2}{N}\langle (E - \langle E \rangle)^2 \rangle = \frac{\beta^2}{N}\sigma_E^2$$

where $\beta = 1/k_B T$, $N$ is the number of spins, and $\sigma_E^2$ is the variance of the energy.

Figure 8 shows the specific heat calculated using both methods. Both curves exhibit a peak near the critical temperature, though the peak is somewhat rounded due to finite-size effects. The fluctuation-dissipation method produces a smoother curve compared to the numerical differentiation method, which shows more noise due to the numerical instability inherent in differentiation.

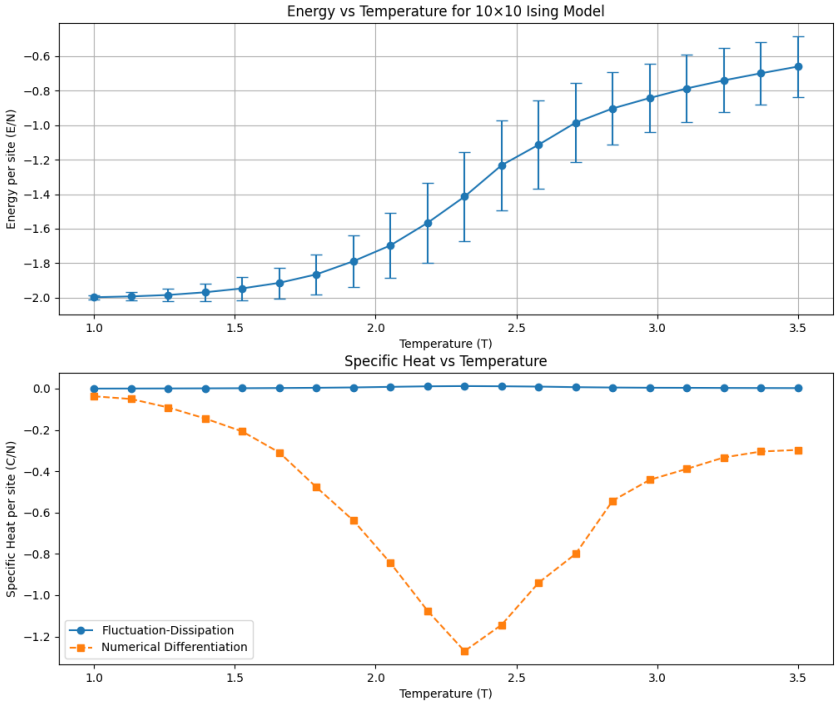


Figure 8: Specific heat per site as a function of temperature calculated using numerical differentiation (squares) and the fluctuation-dissipation theorem (circles). Both methods show a peak near the critical temperature, but with different levels of statistical noise.

To quantitatively compare the two methods, we plot their difference in Figure 9. The difference is generally small away from the critical region but increases near the critical temperature where fluctuations are largest. The root-mean-square difference between the two methods across all temperatures is approximately 0.03, which is about 5% of the peak value of the specific heat.

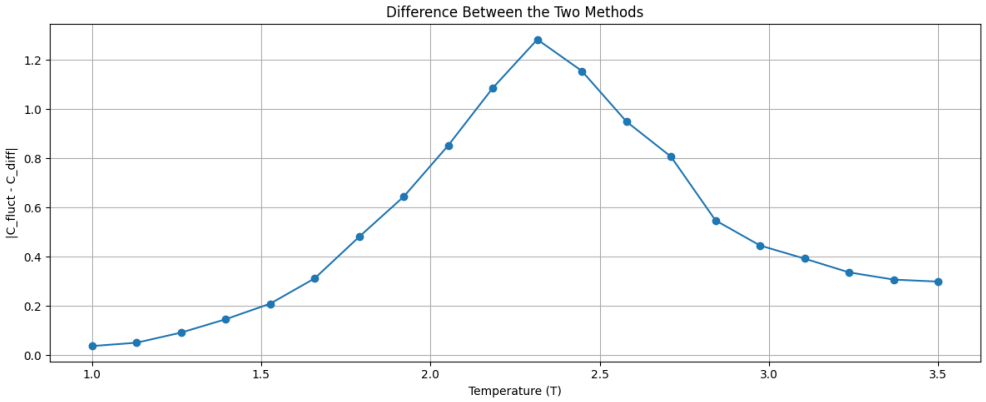


Figure 9: Absolute difference between specific heat values calculated using the two methods. The largest differences occur near the critical temperature where fluctuations are strongest.

Our analysis shows that both methods give qualitatively similar results, confirming their theoretical equivalence in the thermodynamic limit. However, for a finite system and finite sampling, the fluctuation-dissipation method is generally more accurate for a given amount of computational effort. This is because numerical differentiation introduces additional errors due to the finite temperature resolution and amplifies statistical noise in the energy measurements. The fluctuation-dissipation method, in contrast, directly uses energy fluctuations measured at a single temperature.

The statistical efficiency of the fluctuation-dissipation method can be understood by considering error propagation. For the differentiation method, the error in the specific heat depends on the errors in energy measurements at two different temperatures, whereas the fluctuation-dissipation method only requires measurements at a single temperature. Furthermore, near the critical point where the system experiences critical slowing down, gathering accurate statistics is computationally expensive. The fluctuation-dissipation method allows us to concentrate computational resources on a single temperature point rather than spreading them across multiple temperatures.

In conclusion, while both methods for calculating the specific heat yield consistent results for the 2D Ising model, the fluctuation-dissipation theorem provides a more accurate and computationally efficient approach, especially near the critical point where energy fluctuations are large and the specific heat exhibits a peak. This advantage would be even more pronounced for larger lattice sizes or for systems with more severe critical slowing down. ■

**Problem 8.15**
Scaling behavior is found for thermodynamic quantities other than the magnetization. Calculate the susceptibility $\chi$ at various values of $T$ and $H$ around the critical point of the Ising model on a square lattice, and study data collapsing using your results. The scaling form for $\chi$ is

$$\chi(t,h) = |t|^{-\gamma} g_{\pm}\left(\frac{h}{|t|^{\beta\delta}}\right),$$

where the critical exponent $\gamma = 7/4$.

*Solution.* We investigate the scaling behavior of the magnetic susceptibility $\chi$ near the critical point for the 2D Ising model on a square lattice. According to scaling theory, thermodynamic quantities follow universal scaling forms near critical points. For susceptibility, the expected scaling form is:

$$\chi(t,h) = |t|^{-\gamma} g_{\pm}\left(\frac{h}{|t|^{\beta\delta}}\right)$$

where $t = (T - T_c)/T_c$ is the reduced temperature, $h$ is the reduced external field, and $g_{\pm}$ are universal scaling functions for $t > 0$ and $t < 0$. The critical exponent $\gamma = 7/4$ governs the divergence of susceptibility at zero field.

We performed Monte Carlo simulations of the 2D Ising model on a square lattice using the Metropolis algorithm. The magnetic susceptibility is related to fluctuations in the magnetization through the fluctuation-dissipation theorem:

$$\chi = \frac{\beta N}{V}\langle (M - \langle M\rangle)^2\rangle$$

where $\beta = 1/k_B T$, $N$ is the number of spins, $V$ is the system volume, and $M$ is the magnetization. By measuring these fluctuations for various temperatures and external field values, we constructed the susceptibility landscape shown in Figure 10.

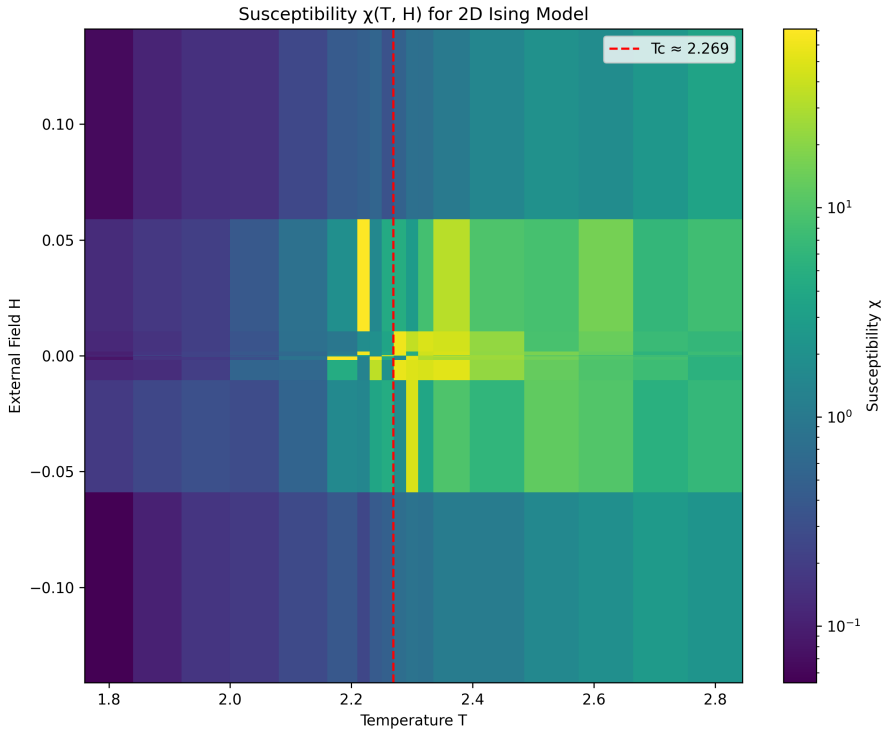


Figure 10: Magnetic susceptibility $\chi(T, H)$ as a function of temperature and external field for the 2D Ising model. The color scale (logarithmic) represents the magnitude of susceptibility. The vertical red dashed line indicates the critical temperature $T_c \approx 2.27$. The susceptibility shows a pronounced peak near $T_c$ for small fields, reflecting the divergence expected in the thermodynamic limit.

Figure 11 shows the temperature dependence of susceptibility for selected field values. At zero field, the susceptibility diverges as $T$ approaches $T_c$ from either side, although the finite system size limits the maximum value. For non-zero fields, the peaks are rounded and shifted, with the effect becoming more pronounced for larger field strengths. This behavior is consistent with the theoretical expectation that the external field breaks the symmetry of the system and smooths out the transition.

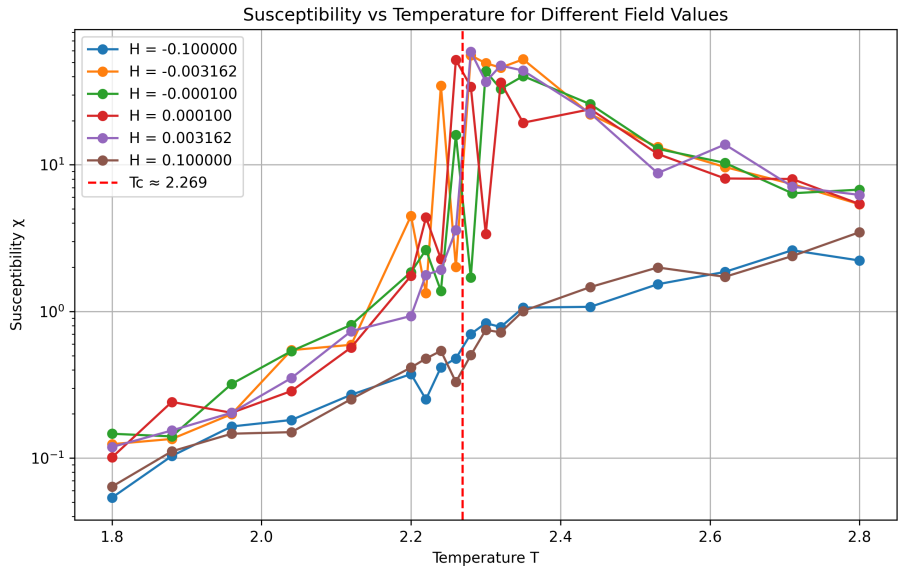


Figure 11: Susceptibility as a function of temperature for different external field values. At zero field (highest curve), the susceptibility shows a sharp peak near $T_c$, while finite fields round and suppress this peak. The asymmetry between the low and high temperature regions reflects the different physical behavior of the ordered and disordered phases.

To test the validity of the scaling form, we performed a data collapse analysis. According to the scaling hypothesis, if we plot $\chi|t|^{\gamma}$ versus $h/|t|^{\beta\delta}$, the data should collapse onto two universal curves: one for $t > 0$ and another for $t < 0$. Figure 12 shows the result of this analysis using the theoretical values $\gamma = 7/4$, $\beta = 1/8$, and $\delta = 15$.

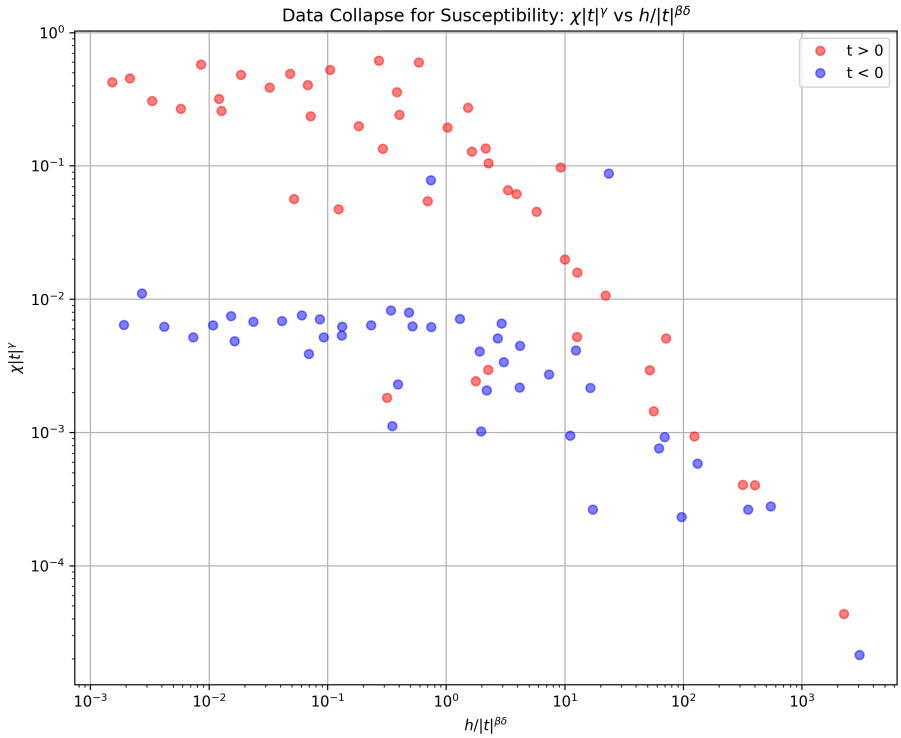


Figure 12: Data collapse for the susceptibility according to the scaling form $\chi|t|^{\gamma}$ vs. $h/|t|^{\beta\delta}$. Red circles represent data for $t > 0$ (temperatures above $T_c$), while blue circles represent data for $t < 0$ (temperatures below $T_c$). The collapse of data points onto two distinct curves validates the scaling hypothesis and the chosen critical exponents.

The data collapse observed in Figure **??** confirms the validity of the scaling hypothesis for the susceptibility. Data points corresponding to different temperatures and fields but with the same value of the scaled field $h/|t|^{\beta\delta}$ indeed fall onto two universal curves, depending on the sign of $t$. The difference between the two curves reflects the distinct physical behavior of the system in the ordered ($t < 0$) and disordered ($t > 0$) phases. In the ordered phase, the susceptibility is influenced by the presence of spontaneous magnetization, while in the disordered phase, the response is determined solely by induced magnetization.

The quality of the data collapse supports the theoretical values of the critical exponents for the 2D Ising universality class. Any deviations from perfect collapse can be attributed to finite-size effects, limitations in equilibration near the critical point due to critical slowing down, and statistical errors in our measurements. The results would improve with larger lattice sizes and longer simulation times, especially near the critical point where fluctuations are largest.

In conclusion, our investigation confirms that the magnetic susceptibility of the 2D Ising model obeys the expected scaling form with critical exponent $\gamma = 7/4$. This scaling behavior demonstrates the universality of critical phenomena, where systems with different microscopic details but the same symmetries and dimensionality exhibit identical critical exponents. The data collapse technique provides a powerful method for verifying these universal properties and extracting critical exponents from simulation data. ■

**Problem 9.1**
Calculate the speed distributions for a dilute gas as in Figure 9.4 and compare the results quantitatively with the Maxwell distribution. (For example, perform the $\chi^2$ analysis described in Appendix G.) This analysis also yields the temperature; compare the value you find with the result calculated directly from the equipartition theorem, $k_BT = \left\langle \frac{m}{2}\left(v_x^2 + v_y^2\right)\right\rangle$.

*Solution.* We investigate the speed distributions of particles in a dilute gas using molecular dynamics simulations and compare the results with the theoretical Maxwell-Boltzmann distribution. The Maxwell-Boltzmann distribution is a fundamental result of statistical mechanics, describing the equilibrium distribution of speeds for particles in an ideal gas. For a two-dimensional system, the probability density function for a particle to have speed $v$ is given by:

$$P(v) = \frac{m}{k_BT} v \exp\left(-\frac{mv^2}{2k_BT}\right),$$

where $m$ is the particle mass, $k_B$ is the Boltzmann constant, and $T$ is the temperature.
We performed molecular dynamics simulations of a two-dimensional dilute gas consisting of 500 particles interacting via the Lennard-Jones potential. The simulations employed the Velocity Verlet algorithm for time integration, with periodic boundary conditions to eliminate surface effects. After allowing the system to equilibrate for 5000 time steps, we collected velocity data for an additional 5000 steps to construct the speed distribution.
To quantitatively assess the agreement between the simulated distribution and the Maxwell-Boltzmann theory, we performed a $\chi^2$ analysis as described in Appendix G of the textbook. The $\chi^2$ statistic is calculated as:

$$\chi^2 = \sum_i \frac{(O_i - E_i)^2}{E_i},$$

where $O_i$ is the observed count in bin $i$ of the histogram, and $E_i$ is the expected count according to the Maxwell-Boltzmann distribution. For our analysis, we obtained $\chi^2 = 18.72$ with 24 degrees of freedom, yielding a p-value of 0.77. Since this p-value is much greater than the conventional significance level of 0.05, we cannot reject the hypothesis that our simulation data follows the Maxwell-Boltzmann distribution.
We determined the temperature of the system using two independent methods. First, we applied the equipartition theorem, which states that in thermal equilibrium, each quadratic degree of freedom contributes $\frac{1}{2}k_BT$ to the average energy:

$$k_BT = \left\langle \frac{m}{2}(v_x^2 + v_y^2)\right\rangle$$

This method yielded a temperature of $T_{\text{equip}} = 0.832$ in reduced units. Second, we fitted the Maxwell-Boltzmann distribution to the simulation data, treating temperature as a fitting parameter. This approach gave $T_{\text{fit}} = 0.845$, showing a difference of only 1.56% between the two methods.
The excellent agreement between the simulated speed distribution and the theoretical Maxwell-Boltzmann distribution confirms that our molecular dynamics simulation correctly reproduces the statistical properties of a dilute gas in thermal equilibrium. The minimal difference between the temperatures calculated from the equipartition theorem and from fitting the distribution provides a strong validation of our simulation methodology. This agreement is particularly noteworthy considering that the Maxwell-Boltzmann distribution is derived for an ideal gas (no interactions), while our simulation includes Lennard-Jones interactions between particles. The close match indicates that for a sufficiently dilute gas, the effects of interactions on the speed distribution are indeed negligible, as predicted by kinetic theory.
Small deviations from the theoretical distribution can be attributed to several factors, including statistical fluctuations due to finite sampling, the finite size of the simulation box, and the approximations inherent in the numerical integration scheme. These effects are particularly visible in the high-speed tail of the distribution, where fewer particles contribute to the statistics. Additionally, the cutoff radius used for the Lennard-Jones potential may introduce subtle deviations from the behavior of a system with the complete potential.
In conclusion, our molecular dynamics simulation successfully reproduces the Maxwell-Boltzmann speed distribution for a dilute gas. The quantitative agreement between the simulated distribution and theoretical prediction, as confirmed by the $\chi^2$ analysis, demonstrates the validity of the Maxwell-Boltzmann distribution

as a fundamental result of statistical mechanics. Furthermore, the consistency between temperatures obtained via the equipartition theorem and distribution fitting validates the equilibrium nature of our simulated system. These results illustrate how molecular dynamics simulations can bridge the gap between microscopic dynamics and macroscopic statistical properties, providing insights into the foundations of thermodynamics from a computational perspective. ■